

# Parametric Studies on Fiber Rebound in Dry-Mix Shotcrete

Vivek Bindiganavile (Contact Author: [vivek@ualberta.ca](mailto:vivek@ualberta.ca))

Department of Civil & Environmental Engineering, University of Alberta, 3-020 NREF Bldg., Edmonton, AB, T6G 2W2, Canada.

For citation information on this paper please see <http://www.claisse.info/specialabstracts.htm>

Nemkumar Banthia

Department of Civil Engineering, University of British Columbia, #2024-6250 Applied Science Lane, CEME Bldg., Vancouver, B.C., V6T 1Z4, Canada

**ABSTRACT** When concrete is sprayed during shotcreting, inevitably some material is lost due to rebound. The relative losses for coarse aggregates and fibers are higher than that for the rest and therefore, the composition of the material in-place is deficient in these phases. In order to compensate for such loss and indeed to minimize it, one must identify the parameters affecting rebound and comprehend the underlying mechanisms. Recent work has established a theory of rebound for coarse aggregates. However, fibers differ from aggregates in their material and geometric properties and the effect of these must be understood in order to extend the existing theory of rebound to fibers. This is a study on the influence of particle density upon the rebound of a projectile impinging via the dry-mix process onto fresh shotcrete. The empirical model developed in this study postulates that a lower aggregate density favours lower rebound and this prediction was verified using two kinds of lightweight aggregates in dry-mix shotcrete.

## INTRODUCTION

Shotcrete in general and dry-mix shotcrete in particular is characterized by a significant loss of material that ricochets off the target substrate. This phenomenon is termed as rebound and as a result, the in-place mix constituents differ in proportion to the original mix design. In addition to the economic losses incurred during rebound, the altered mix results in vastly different mechanical properties for the in-place material in comparison to the one designed. Nowhere is this more relevant than with fibers, which are introduced to the mix for imparting flexural toughness. Where as aggregates are seen to rebound about 20-30 % during shotcreting (Austin & Robins, 1995), considerably higher figures are noticed for fibers, with steel fibers rebounding at 35-78 % (Morgan *et al.*, 1987; Banthia *et al.*, 1992). No data exists in the literature on rebound of polymeric macro-fibers; however, in unpublished data from tests done at the University of British Columbia, rebound values in the range of 40-90 % have been observed. Clearly, with such high losses in rebound, the material in-place is very poorly reinforced from the toughness point of view. Fibers being relatively expensive, the rebound phenomenon in turn implies a high financial loss, particularly with the dry-mix process. Hence, their use in the field of dry-mix shotcrete has been undermined by the huge rebound losses.

In this light, it is important to understand the reasons behind the high fiber rebound associated with the dry-mix shotcrete process. Where as recent research has developed a theory for the rebound of aggregates (Armelin, 1997), a similar understanding of the mechanism of fiber rebound is desired. The authors began by recognizing that fibers and aggregates differ considerably in their material and geometric characteristics. Therefore, in order to describe the phenomenon of fiber rebound, it was deemed necessary to study the effect of certain material and geometric parameters of a projectile impinging upon a fresh shotcrete substrate. Where as the density of normal aggregates is close to that of fresh shotcrete, typical fibers are made of polymers, cellulose and steel, with densities very different from that of fresh shotcrete. Hence, in this report, the effect of density has been isolated as a key material parameter. Since the theory of aggregate rebound is based on a model for spherical projectiles, it was decided that the material influence on rebound should be studied upon spheres of identical size, differing only in their density. In addition, the present study was conducted upon three different sphere diameters to allow for investigating the effect of density over a range of sizes. Accordingly, spheres made of eight different materials with densities between 600 kg/m<sup>3</sup> (wood) to 14,950 kg/m<sup>3</sup> (tungsten carbide) and in three sizes (9.53 mm, 12.70 mm & 25.40 mm), were chosen for

this study. The materials and sizes chosen allowed the authors to verify the already established theory of aggregate rebound and extend it to describe the effect of density on the rebound of a spherical projectile from fresh shotcrete.

## THEORETICAL BACKGROUND

A detailed description of a model for aggregate rebound was given by Armelin and Bantia (1998a-b). This model extends the already established theories surrounding impact of a metallic projectile onto a metallic substrate with suitable modifications made to account for the rheology of fresh shotcrete. The mechanism of rebound of a spherical projectile from fresh shotcrete may be divided into three phases namely, a) translation in flight, b) penetration upon impact and c) the reaction phase during which it may either stay embedded or rebound. The phenomenon is thought to proceed as follows: A projectile penetrates due to its kinetic energy prior to impact. The cavitation caused during penetration results in elastic strain energies developed within both the projectile and the substrate, which is then released. This energy is transferred back to the projectile imparting it with a reactionary kinetic energy that may cause it to rebound. Since the phenomenon of rebound exists, the usual idealization of fresh shotcrete as a Bingham fluid (Tattersall & Banfill, 1983; Ghio, 1993; Beaupré, 1994) is not entirely valid because if it were so, there would be no elastic component to fresh shotcrete rheology thereby eliminating any possibility of an impinging particle ricocheting from the surface. Therefore, the model is based upon assuming that fresh shotcrete is an elasto-plastic substrate, which obeys the Tresca yield-criterion.

### *Translation in flight*

A projectile when given a velocity 'V' follows a parabolic path in flight as it approaches the target. If the projectile possesses high flexural rigidity, it may be idealized as a particle (which is the basis for this model) with no loss in kinetic energy through bending in flight.

### *Penetration phase*

As a spherical projectile approaches the target, due to its velocity 'V<sub>imp</sub>' just prior to impact, it possesses a kinetic energy with which it penetrates into the

substrate and causes a cavitation. The work done in penetrating is estimated as follows.

Due to the radial symmetry of the displacements during penetration, it may be assumed that below the contact surface, a hemispherical core is formed in which a hydrostatic state of pressure ( $p$ ) exists. As described in Figure 1, the region  $r < a$  depicts the cavity while in the region  $a < r < c$ , an elasto-plastic state of stress exists. Beyond the elasto-plastic boundary ( $r = c$ ), no plastic flow occurs and the theory of elasticity may be applied. Therefore, the boundary conditions for the state of stress are:

1. Since the hemispherical cavity is in a hydrostatic state of stress, ' $p$ ', and stress in the radial direction, ' $\sigma_r$ ', is in the principal direction, on the surface of the cavity, we have:

$$\sigma_r|_{(r=a)} = p \quad \dots(1)$$

2. In the plastic region, the radial stresses are given by Hill (1950), assuming the Tresca yield-criterion. Thus, for the yield strength of the medium  $Y$ , we have in the region ( $a \leq r \leq c$ ):

$$\frac{\sigma}{Y} = -2 \ln\left(\frac{c}{r}\right) - \frac{2}{3} \quad \dots(2)$$

3. In the elastic zone, we have:

$$\frac{\sigma_r}{Y} = -\frac{2}{3} \left(\frac{c}{r}\right)^3 \quad \dots(3)$$

For compatibility, displacements at the boundary of the core (=  $da$ ) must accommodate the volume displaced by the projectile. With the above boundary conditions and invoking the condition of compatibility, we obtain the solution for the contact stress ( $p$ ):

$$\frac{p}{Y} = \frac{2}{3} \left\{ \ln\left(\frac{aE}{3RY}\right) + 1 \right\} \quad \dots(4)$$

Armelin (1997) interprets this result to indicate that for fresh shotcrete, the stress acting on the surface of an aggregate as it penetrates into the substrate is constant throughout the contact region. Therefore, the work done in penetration by the contact stress, ' $p$ ' may now be equated to the kinetic energy of the aggregate at impact,  $W_1$ . Thus, if  $v_{cav}$  is the volume of the cavity:

$$\frac{1}{2} m V_{imp}^2 = W_1 = p v_{cav} \quad \dots(5)$$

Note that the above formulation assumes a quasi-static stress state during penetration. However, as indicated by previous studies (Tattersall & Banfill, 1983; Ghio, 1993; Beaupré, 1994), fresh concrete is a strain-rate sensitive material and hence the penetration event is a time-dependent one. Which is

why, the contact stress in Equation (5) shall have to be replaced by a dynamic contact stress, ' $p_d$ '. So that,

$$\frac{1}{2}mV_{imp}^2 = p_d V_{cav} \quad \dots(6)$$

### Reaction Phase

The penetration of the projectile into the fresh shotcrete induces strain energy in both the projectile and the substrate, which is transferred to the projectile after full penetration. This results in a kinetic energy, ' $W_2$ ', that may eventually eject the projectile out in the form of rebound. The relative values of the impacting kinetic energy, ' $W_1$ ' and the rebound energy ' $W_2$ ' determine the tendency for a particular projectile impact event to result in rebound.

The calculation of rebound energy begins by recognizing that when the projectile is ejecting out, the cavity it leaves is in fact larger than the one it originally occupied. This is because the ejection is a result of elastic "spring-back" of the fresh material surrounding the projectile. Therefore, the rebound energy may be calculated as the work done to shrink the large cavity to come into contact with the spherical projectile. Being an elastic process, it may be calculated as the work done by a force, ' $f$ ', which pushes the projectile through a distance, ' $z^*$ ', during which the cavity increases in radius from ' $a$ ' to ' $a^*$ '. Thus, in a direction ( $z$ ) along the path of the projectile inside the substrate,

$$W_2 = \int_0^{z^*} f(z) dz \quad \dots(7)$$

This was solved to yield:

$$W_2 = \frac{3\pi^2}{10} p^2 a^{*3} \left[ \frac{1-\nu_c^2}{E_c} + \frac{1-\nu_i^2}{E_i} \right] \quad \dots(8)$$

where, ' $E_c$ ', ' $\nu_c$ ' and ' $E_i$ ', ' $\nu_i$ ' are the elastic constants for the composite and the impactor respectively.

We may note here that the coefficient of restitution, ' $e$ ', is a measure of the ratio of the rebound and impacting kinetic energies, for:

$$e = \frac{V_r}{V_{imp}} = \sqrt{\frac{W_2}{W_1}} \quad \dots(9)$$

After conceding that the elastic modulus of the impactor is several orders of magnitude higher than that of the substrate, Armelin & Banthia (1998a) obtained the following expression for the coefficient of restitution:

$$e = \sqrt{\frac{3\pi^2}{10} \left(\frac{4r_1}{\pi}\right)^{3/4} \left(\frac{1}{E^*}\right) \left(\frac{1}{2}m\right)^{-1/4}} \cdot p \cdot (p_d)^{-3/8} \cdot V_{imp}^{-1/4} \quad \dots(10)$$

For the case of spheres made of the same material, the above expression may be simplified as:

$e = K \psi$ , where, ' $K$ ' is a constant,

$$K = \sqrt{\frac{3\pi^2}{10} \left(\frac{4r_1}{\pi}\right)^{3/4} \left(\frac{1}{E^*}\right) \left(\frac{1}{2}m\right)^{-1/4}} \quad \text{and}$$

$$\psi = p \cdot (p_d)^{-3/8} \cdot V_{imp}^{-1/4}$$

The quantity, ' $\psi$ ', known as the "impact factor", is a measure of the rebound tendency for each spherical particle.

However, because in the present study, spheres of different materials and hence various densities were tested, we may express the coefficient of restitution in terms of a constant, ' $K'$ ', and the *modified impact factor* ' $\psi^*$ ' such that,

$$K' = \sqrt{\frac{3\pi^2}{10} \left(\frac{4r_1}{\pi}\right)^{3/4} \left(\frac{1}{E^*}\right) \left(\frac{1}{2}v\right)^{-1/4}} \quad \dots(11)$$

$$\text{and } \psi^* = \rho^{-1/8} \cdot p \cdot (p_d)^{-3/8} \cdot V_{imp}^{-1/4} \quad (12)$$

where,

$v$  = the volume of the impactor; and,  
 $\rho$  = density of the projectile material.

The modified impact factor gives us a measure of relative tendencies of rebound for different projectile-substrate combinations. In the present study, the  $\psi^*$  values for spheres of different densities and radii have been calculated to understand the effect of material parameters upon rebound.

## EXPERIMENTS AND METHODS

Spherical projectiles ranging from 9.53 mm to 25.40 mm in diameter (3/8 inch to 1 inch) and ranging in density from 600 kg/m<sup>3</sup> to 14,950 kg/m<sup>3</sup> were chosen for impact measurements on fresh concrete. Table 1 presents a description of the spheres investigated.

In order to study the effect of projectile density on rebound, the spheres described in Table 1 were propelled by the dry-mix shotcreting machine ALIVA 246 (Figure 2) in conditions identical to that during actual shotcreting. Thus, each sphere was supplied with a pressure of 300 PSI (2.07 MPa) as it emerged from the nozzle. A panel of fresh concrete

was placed at a distance of 750 mm from the nozzle, in the manner shown in Figure 3. Since the bigger and/or heavier spheres were much slower than the rest, the distance of 750 mm was chosen through trial and error in order to ensure contact between every projectile and the target substrate for this experiment. (For instance, heavier ones like those of tungsten carbide would not even reach the target at distances beyond 750 mm.)

The yield resistance of the freshly cast concrete substrate was determined through a digital penetrometer with a 9 mm diameter needle (Figure 4). A few sample plots of resistance versus the distance of penetration are shown in Figure 5. Cast concrete offers a resistance of ~ 0.50 MPa as opposed to dry-mix shotcrete, which in this study had a consistency corresponding to resistance of 2 ( $\pm$  0.5) MPa.

### Calculations

The purpose of conducting impact measurements on fresh concrete, one sphere at a time, was to estimate the velocity of impact and to calculate the volume of indentation for each sphere. This was used to calculate the dynamic contact stress, ' $p_d$ '. Several trials (a minimum of five) were conducted with each sphere in order to evaluate the distance travelled in space, ' $S$ ', due to an initial pressure, ' $P$ ', of 300 PSI (2.07 MPa). For each sphere, the force applied due to the initial air pressure, ' $F$ ', was calculated as the product of the pressure, ' $P$ ', and the projected area, ' $A$ '. Thus,

$$F = P \times A \quad \dots(13)$$

The work done on the sphere, ' $W_i$ ' was calculated as the product of the force applied, ' $F$ ', and the distance travelled, ' $S$ ', so that

$$W_i = F \times S \quad \dots(14)$$

Thus, the initial kinetic energy supplied to every sphere was:

$$\left(\frac{1}{2}\right)mV^2 = F \times S \quad \dots(15)$$

Since the fresh concrete target was placed at a distance of 750 mm from the nozzle, the kinetic energy at impact is given by,

$$\left(\frac{1}{2}\right)mV^2 - \left(\frac{1}{2}\right)mV_{imp}^2 = F \times 750 \quad \dots(16)$$

But,

$$\left(\frac{1}{2}\right)mV^2 = F \times S \quad (\text{from Equation (15)}).$$

Therefore,

$$\left(\frac{1}{2}\right)mV_{imp}^2 = F(S-750)$$

and the velocity at impact is given by:

$$V_{imp} = \sqrt{\frac{2F}{m}(S-750)} \quad \dots(17)$$

The dynamic contact stress, ' $p_d$ ', is calculated as follows:

If ' $v_{cav}$ ' is the volume of indentation created by a sphere, work done by the sphere is equal to the product of the dynamic contact stress and the volume of indentation.

Thus,

$$\left(\frac{1}{2}\right)mV_{imp}^2 = p_d v_{cav} \quad \dots(18)$$

So that,

$$p_d = \frac{\left(\frac{1}{2}\right)mV_{imp}^2}{v_{cav}} \quad \dots(19)$$

Knowing the projectile density, ' $\rho$ ', the static contact stress, ' $p$ ' (from experimental results as in Figure 5), the dynamic contact stress, ' $p_d$ ' (from Equation (19)), and the velocity at impact, ' $V_{imp}$ ' (from Equation (17)), we may now proceed to calculate the modified impact factor, ' $\psi^*$ ' as per Equation (12).

## RESULTS AND DISCUSSIONS

The velocity at impact, ' $V_{imp}$ ', for the different spheres projected on to a fresh concrete substrate, are plotted in Figure 6. Note that the smaller spheres had a higher velocity as did those having a lower density. Figure 7 describes the modified impact factor, ' $\psi^*$ ', for all spheres as a function of their density. While smaller spheres had lower values of ' $\psi^*$ ', a linear increase with density was noted at all sizes. The effect of particle size on the modified impact factor is described for steel balls in Figure 8. An increase in the values of ' $\psi^*$ ' is noted, which is in keeping with earlier observations (Armelin and Banthia, 1998a-b) that bigger projectiles tend to result in higher rebound.

In order to verify the findings in this study, three shotcrete mixes containing coarse aggregates of varying densities were sprayed into panels via the dry-mix process. The mixes were shot onto wooden forms (600 mm x 500 mm x 100 mm) with tapered sides inside a closed shooting chamber as shown in Figure 9, using a 350 cu ft/min air-flow (1 cu ft/min = 0.5 m<sup>3</sup>/s). The physical properties of aggregates used in this study are listed in Table 2 while the shotcrete mix designs are given in Table 3<sup>1</sup>. Note

<sup>1</sup> It should be noted that unlike for cast concrete (or shotcrete sprayed via the wet-mix process), in the dry-mix process, the water is added towards the end of the stream and as such the control of the water content rests solely with the nozzleman who falls back upon his experience and judgement. Hence, the

that over 95% of the particles for all aggregate types, were in the 2-10 mm range. The overall rebound values are shown alongside. Note that a progressively higher rebound was registered with an increase in the density of the aggregate particles. As the coarse aggregates were added based on equal weight measures and not on equal volume measures, increasingly larger volumes were incorporated for expanded clay and pumice aggregates. Even so, the overall rebound with lightweight aggregates was less than that for mixes with normal weight aggregates, which attests to the prediction using modified impact factors.

From investigating fiber rebound in dry-mix shotcrete, it is apparent that all fibers cannot be clubbed together under the umbrella of a single model. This is clear from the data on micro-fibers of polypropylene, which clearly show a much lower rebound than the macro fibers of the same material (UBC Report, 2000). In fact, the rebound of micro-polymeric fibrils was seen to be only as much as that of the overall rebound. Therefore, it appears that where as macro-fibers travel as individual particles in the dry-mix shotcrete stream, micro-fibers especially those that disperse well, are well assimilated with the fines and hence do not result in high rebound.

Although the rebound tendency for lightweight aggregates was in keeping with the prediction from the modified theory of rebound emerging out of this study, it does not explain the response of macro fibers, typically used in shotcrete. For, it has long been known that although steel is heavier than polypropylene (by nearly an order of magnitude), the rebound of polymeric macro-fibers is much higher than that of steel macro-fibers. The authors believe that both density and flexural rigidity influence rebound of a macro-fiber in dry-mix shotcrete. Research is ongoing in order to extend the theory of rebound further to include the flexural rigidity of the projectile. Nevertheless, the findings in this study offer tremendous potential for the optimization of mix design, including the use of locally available lightweight aggregates and the choice of fiber materials.

## CONCLUSIONS

The following conclusions may be drawn from the present study:

---

water content was assessed indirectly after the material was shot into place, by measuring separately the water and binder contents.

1. The theory of aggregate rebound in dry-mix shotcrete may be extended to include projectiles of various densities. Using spheres of 8 different materials with a range of densities from 600 to 15000 kg/m<sup>3</sup>, it was seen that the proposed model predicts that higher densities will lead to a higher tendency of rebound.
2. The model developed here was verified using three types of aggregates having densities from 700 kg/m<sup>3</sup> to 2670 kg/m<sup>3</sup>. Upon shotcreting via the dry-mix process, the overall rebound was seen to increase with an increase in the aggregate density.
3. As previously noted, the rebound of larger particles was higher than that of smaller ones. This was verified for three different sphere diameters across a wide range of projectile materials.

## NOTATIONS

$c$	= radius of the elastic boundary formed around the hydrostatic core;
$e$	= coefficient of restitution;
$E_c, E_i$	= composite and impactor modulus of elasticity;
$K, K'$	= Constants relating the coefficient of restitution to the impact factor (and the modified impact factor);
$m$	= mass of the impactor;
$V, V_{imp}$	= initial and impacting velocity of the impacting projectile;
$W_1, W_2$	= energy of impact and rebound;
$Y$	= yield stress of the substrate as determined by uniaxial stress conditions;
$a$	= radius of contact area made between the impactor and the substrate;
$a^*$	= maximum radius of the contact area made during the penetration phase;
$p, p_d$	= static and dynamic contact stress between the impactor and the substrate;
$V_{cav}$	= volume of cavitation indented by the impactor;
$\delta$	= depth of penetration by the impactor;
$\delta^*$	= maximum depth of penetration during the entire penetration phase;
$\rho$	= density of the impactor;
$\sigma_r$	= radial component of stress acting on the substrate;
$\psi, \psi^*$	= impact factor and the modified impact factor (for variable projectile density).

## ACKNOWLEDGEMENTS

The authors would like to thank Synthetic Industries (Chattanooga, TN) and NSERC, Canada for funding part of the research presented here. The authors gratefully acknowledge the support from Mr. Rodney Hicks (Lehigh Cement Company, Vancouver, BC) and Mr. Garth Carefoot (Great Pacific Pumice Inc., Vancouver, BC) for supplying the lightweight expanded clay and pumice aggregates, respectively. In addition, the assistance of Mr. Fariborz Madjzadeh and Mr. David Woo in conducting the experiments is much appreciated.

## REFERENCES

Armelin, H.S. (1997). "Rebound and toughening mechanisms in steel fiber reinforced dry-mix shotcrete", Ph.D. Thesis, The University of British Columbia, 262 pages.

Armelin, H. S. and Banthia, N. (1998a). "Mechanics of aggregate rebound in shotcrete – (Part 1)", *Materials and Structures*, Vol. 31, March, pp. 91-98.

Armelin, H. S. and Banthia, N. (1998b). "Development of a general model of aggregate rebound in dry-mix shotcrete – (Part 2)", *Materials and Structures*, Vol. 31, April, pp.195-202.

Austin, S. A. and Robins, P. J. (1995). "Sprayed concrete: Properties, design and application", Whittles Publishing, page 41.

Banthia, N., Trottier, J-F., Wood, D. and Beaupré, D. (1992). "Influence of fiber geometry in steel fiber reinforced dry-mix shotcrete", *ACI Concrete International*, Vol. 14, no. 2, pp. 24-28.

Beaupré, D. (1994). "Rheology of high-performance shotcrete", Ph.D. Thesis, The University of British Columbia, 250 pages.

Ghio, V. (1993). "The rheology of fresh concrete and its effects on the shotcrete process", Ph.D. Thesis, The University of California, Berkeley, 193 pages.

Hill R. (1950). "The mathematical theory of plasticity", Oxford University Press, London, UK, page 99.

Morgan, D. R., McAskill, N., Neill, J. and Duke, N. F. (1987). "Evaluation of silica fume shotcretes", *Proceedings of CANMET/ACI Workshop on Condensed Silica Fume in Concretes*, Montreal, page 34.

Tattersall, G. H. and Banfill, P. F. G., (1983). "The rheology of fresh concrete", Pittman Publishing, 356 pages.

UBC Report, 'Use of polymeric micro-fibers in shotcrete', September 2000.

Table 1 Properties of Spheres Investigated in this Study

Diameter (mm)	Material	Density (kg/m <sup>3</sup> )
9.53	Polypropylene	900
9.53	Teflon	2400
9.53	Ceramic	3600
9.53	Steel	7800
9.53	Brass	8400
9.53	Tungsten Carbide	14950
12.70	Wood	600
12.70	Ceramic	3600
12.70	Steel	7800
25.40	Polypropylene	900
25.40	Lucite	1300
25.40	Steel	7800

Table 2 Properties of Aggregates Investigated in this Study

Normal Weight Aggregate			Expanded Clay Aggregate			Pumice Aggregate		
Density	Gradation		Density	Gradation		Density	Gradation	
kg/m <sup>3</sup>	Sieve Size (mm)	% Retained	kg/m <sup>3</sup>	Sieve Size (mm)	% Retained	kg/m <sup>3</sup>	Sieve Size (mm)	% Retained
2670	9.423	4.95	1200	9.423	31.77	700	9.423	5.35
	4.750	97.90		4.750	87.65		4.750	68.60
	1.998	100		1.998	96.50		1.998	97.52
	1.180	100		1.180	97.39		1.180	98.53
	0.590	100		0.590	98.04		0.590	99.06
	0.297	100		0.297	98.46		0.297	99.47
	0.147	100		0.147	99.58		0.147	99.73

Table 3 Details for the Shotcrete Mixes as Batched

Mix no.	Cement (kg/m <sup>3</sup> )	Sand (kg/m <sup>3</sup> )	Coarse Aggregate (kg/m <sup>3</sup> )	Water/Binder Ratio <sup>†</sup>	Silica Fume (kg/m <sup>3</sup> )
1 (Normal)	393	1490	370	0.40	44
2 (Ex. Clay)	393	1490	370	0.43	44
3 (Pumice)	393	1490	370	0.48	44

<sup>†</sup> The water/binder ratio was determined after the panel was shot. Approximately 2 kg sample of the material in-situ was heat dried to determine the water content. The binder fraction in the fresh shotcrete was assessed by washing a similar amount using a 200 µm screen.



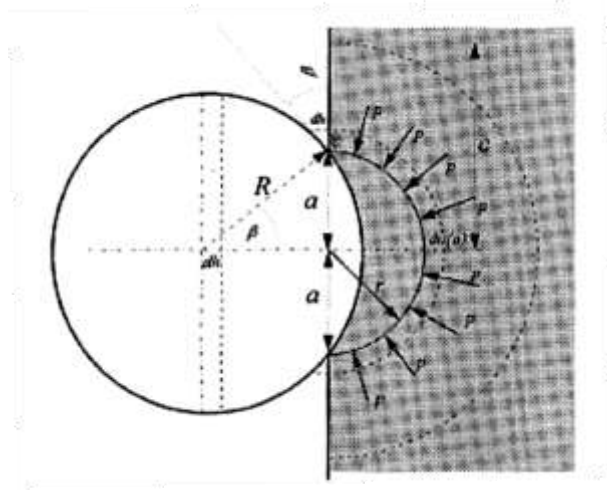
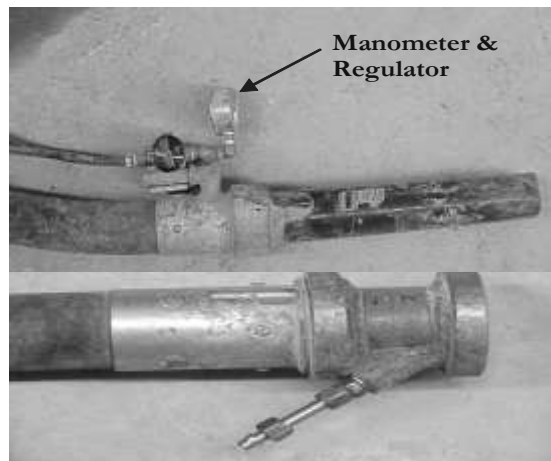


Figure 1 Spherical Projectile Striking the Elasto-Plastic Surface with the Formation of a Hydrostatic Cavity ( $r < a$ ) and the Elasto-Plastic Region ( $r < c$ ) [after Armelin, 1997].



a)



b)

Figure 2 The Mixes were Shot at the University of British Columbia using (a) ALIVA 246: Dry-Mix Shotcrete Machine, with a (b) Brazilian Ring to Control the Water Dosage

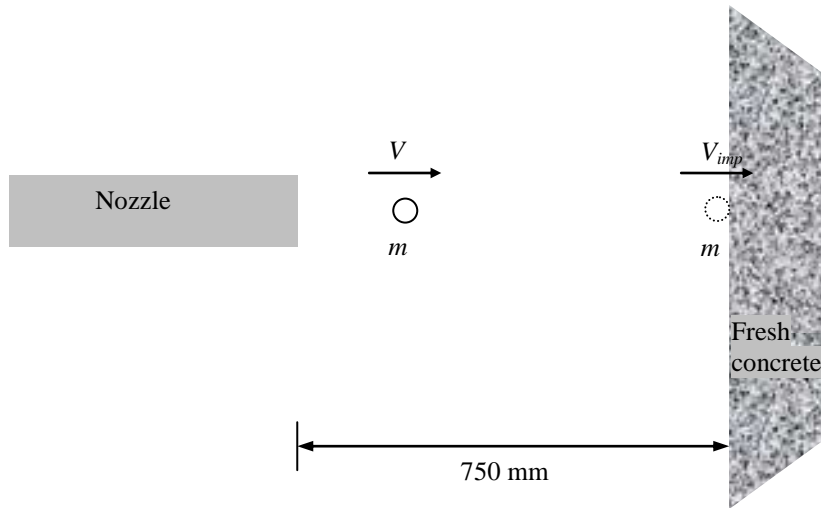


Figure 3 Schematic of Set-Up to Determine the Volume of Indentation

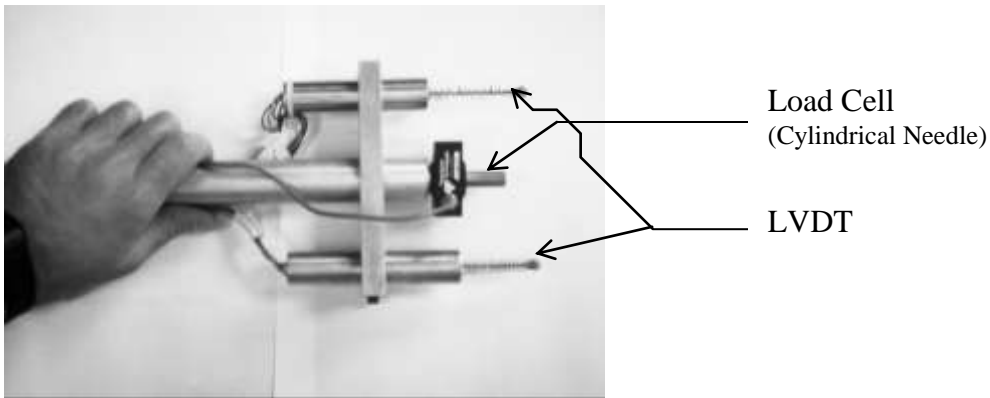


Figure 4 Digital Penetrometer for Evaluating the Consistency of Fresh Shotcrete

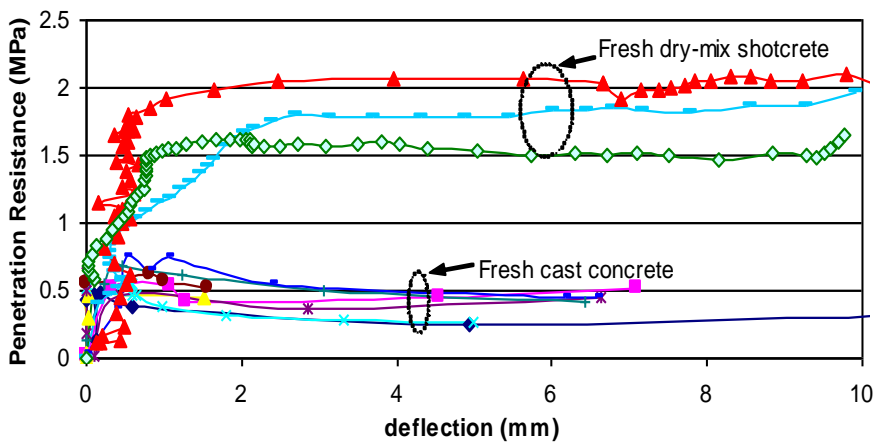


Figure 5 Penetration Resistance of Fresh Concrete and Dry-Mix Shotcrete

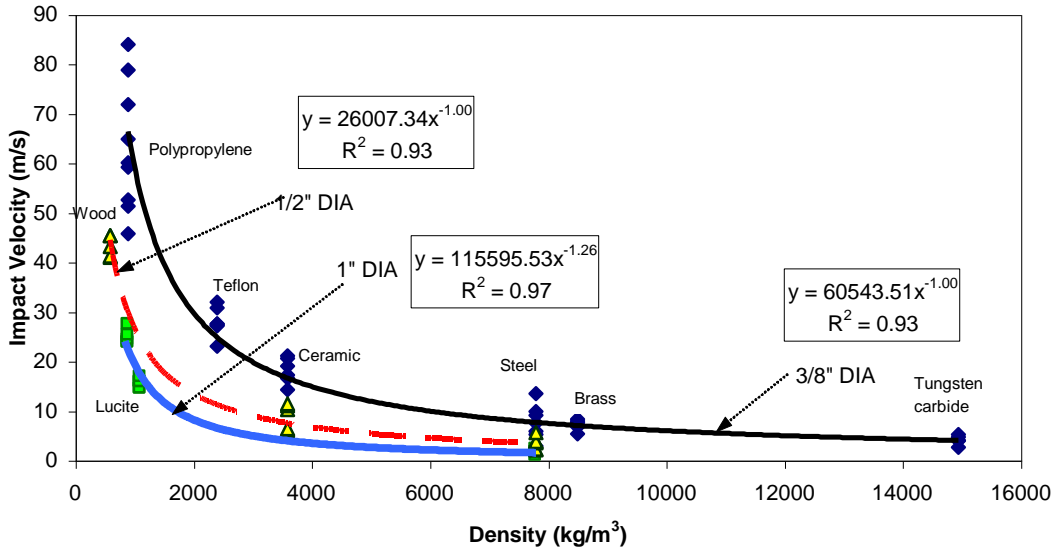


Figure 6 Impact Velocity for Various Spheres as a Function of their Density

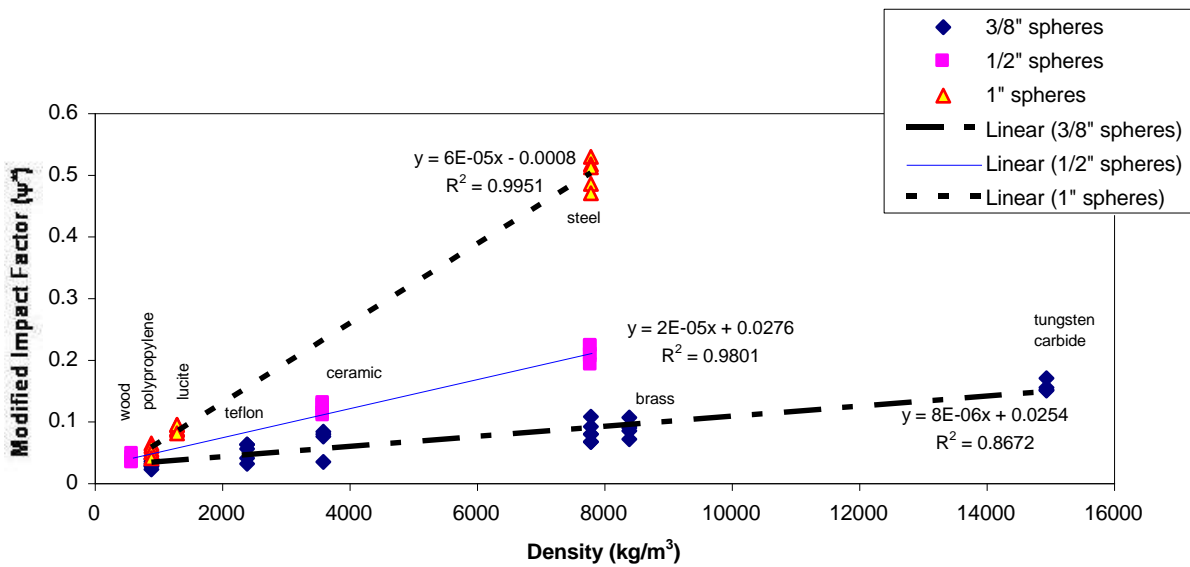


Figure 7 Modified Impact Factor ( $\psi^*$ ), which Describes the Possibility of Rebound as a Function of Projectile Density for Three Sphere Sizes

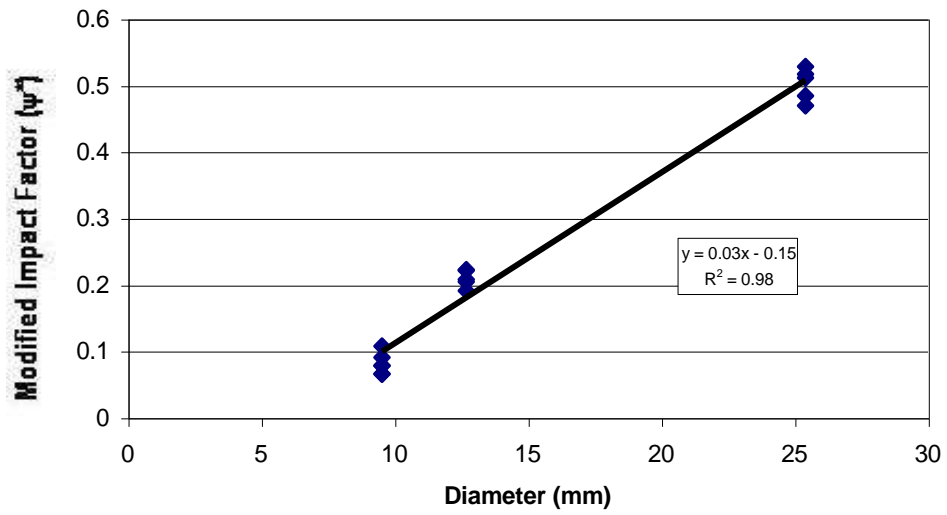


Figure 8 Effect of Particle Size on the Rebound Tendency as Expressed by the Modified Impact Factor ( $\psi^*$ ) for Steel Spheres



Figure 9 Shotcreting in Progress